DOI: 10.1002/cmdc.200600037

Phosphopeptide Ligands of the SHP-1 N-SH2 Domain: Effects on Binding and Stimulation of Phosphatase Activity

Kornelia Hampel,[a] Ina Kaufhold,[a] Martin Zacharias,[b] Frank D. Böhmer,[c] and Diana Imhof*[a]

*Src homology 2 (SH2)-domain-mediated interactions with phosphotyrosine (pY)-containing ligands are critical for the regulation of SHP-1 phosphatase activity. Peptides based on a binding site from receptor tyrosine kinase Ros (EGLN-pY2267-MVL, **1**) have recently been shown to bind to the SHP-1 N-terminal SH2 domain (N-SH2) with considerably high affinity. In addition, two peptides cyclized between positions −1 and +2 relative to pY (EGLc[K-($COCH_2$NH)pYMX]L-NH_2, **2**: X=D, **3**: X=E) bound to the N-SH2 domain, but did not activate the enzyme and even partially prevented stimulation of SHP-1 activity by the physiological ligand **1**. These findings prompted us to further examine the determinants for optimal binding to the N-SH2 domain and for the stimulation and inhibition of SHP-1 activity. Herein we demonstrate that combining the preferred residues in both pY+1 (such as Phe or norleucine, Nle) and pY+3 (such as homophenylalanine, Hfe) leads to highly efficient activating ligands of SHP-1. Particularly in the context of the cyclic peptides **7** (EGLc[K-($COCH_2$NH)pYFD]Hfe-NH_2) and **8** (EGLc[K($COCH_2$NH)pYNleD]HfeL-NH_2), the incorporation of these residues resulted in high-affinity ligands with a significantly increased ability to stimulate SHP-1 activity. We suggest that different binding modes (according to consensus sequences class I and II) are responsible for obtaining either activating (**7** and **8**) or nonactivating (**2** and **3**) ligands. Peptides such as **7** and **8** that bind in the extended fashion of the type II mode activate the phosphatase through complete filling of the cavity for pY+3. In contrast, peptides such as **2** and **3** that bind in the class I mode do not activate the enzyme because they allow more conformational space at pY+3. Therefore, their binding does not force the conformational transition necessary to trigger the dissociation of N-SH2 and the catalytic domain.*

Introduction

Protein tyrosine phosphorylation and dephosphorylation are critical in regulating processes such as cell growth, cell-cycle regulation, and cell differentiation.[1,2] Several protein tyrosine phosphatases (PTPs) were shown to be associated with human diseases.[3] Thus, the interest in PTPs as drug targets for regulating signaling pathways has increased over the past decade.[4]

The cytosolic PTP, SHP-1, consists of two SH2 (Src homology 2) domains at the N terminus, followed by a catalytic domain (PTP domain) and a short C-terminal tail.[5] SHP-1 is predominantly expressed in hematopoietic cells and at a lower level in epithelial cells.[6] The investigation of the phenotype of mice containing mutations in the SHP-1 gene provided insight into the function of SHP-1. The absence of SHP-1, as in the motheaten (*me*/*me*) mouse strain, or the expression of a catalytically defective SHP-1, as in viable motheaten (me^v/me^v) mice results in severe immunodeficiency, which leads to patchy dermatitis, extramedullary hematopoiesis, splenomegaly, hemorrhagic pneumonitis, and sterility.[7–9] Investigation of these mice demonstrated the involvement of SHP-1 in multiple stages of hematopoietic development, and it allowed the identification of target proteins, guided by their elevated phosphorylation in cells isolated from *me*/*me* and me^v/me^v mice.[10,11] Altered SHP-1 levels are also associated with different diseases in humans. For example, increased protein levels of SHP-1 in neutrophils have been found in severe congenital neutropenia.[12] Furthermore, gene silencing by aberrant methylation of the SHP-1/PTPN6 gene, and alternative splicing resulting from base modifications by hyperediting are associated with acute myeloid leukemia, lymphomas, and multiple myelomas. In addition, low SHP-1 levels may be related to enhanced activity of mitogenic and antiapoptotic signaling pathways in the corresponding tumor cells.[13–15] Thus, the importance of SHP-1 in a wide range of signal transduction pathways, and its association with the pathogenesis of various diseases explains the great interest in generating effectors of SHP-1 phosphatase activity. Further-

[a] *K. Hampel, I. Kaufhold, Dr. D. Imhof*
Institute of Biochemistry and Biophysics
Biological and Pharmaceutical Faculty, Friedrich Schiller University
Philosophenweg 12, 07743 Jena (Germany)
Fax: (+49) 3641-949352
E-mail: Diana.Imhof@uni-jena.de

[b] *Prof. Dr. M. Zacharias*
International University Bremen School of Engineering and Science
Campus Ring 8, 28759 Bremen (Germany)

[c] *Prof. Dr. F. D. Böhmer*
Institute of Molecular Cell Biology
Medical Faculty, Friedrich Schiller University
Drackendorfer Str. 1, 07745 Jena (Germany)

more, selective effectors of SHP-1 may be useful tools for the further characterization of the cellular functions of this enzyme.

The SH2 domains of SHP-1 play an important role in the regulation of enzyme activity. In the absence of stimulus, SHP-1 is inactive through allosteric inhibition by its N-terminal SH2 (N-SH2) domain.[5] The binding of a phosphotyrosine (pY)-containing ligand leads to a conformational shift within the N-SH2 domain, upon which the PTP domain is released and made accessible for substrate molecules.[5,16] In contrast, the C-SH2 domain is highly flexible and has been suggested to act as a recruiting unit for ligand binding to the N-SH2 domain.[5,17] SHP-1 can also be activated efficiently by simultaneous engagement of both SH2 domains by bisphosphorylated peptides; this occurs in immunoreceptors containing several ITIMs (immunoreceptor tyrosine-based inhibitory motifs). This association was shown to be more efficient than that obtained with monophosphorylated peptides.[18] In addition, the activation of SHP-1 by the association of acidic phospholipids to the C-terminal tail, and to a lesser extent the N-terminal SH2 domain motif, has been reported.[19] Another mechanism of SHP-1 activation involves two tyrosine residues at the C terminus that can be phosphorylated by several PTKs such as *c*-Src. Phosphorylation of Y536 (Y538 in the epithelial variant) leads to an association with the N-SH2 domain in an intramolecular fashion, and thus to a relief of the basal inhibition. In contrast, the phosphorylated Y564 (or Y566) site has the potential to occupy the C-SH2 domain, and thus to influence the catalytic activity of SHP-1.[20] These mechanisms of SHP-1 activation may play a role in the absence of efficient ligands for the N-terminal SH2 domain.[21]

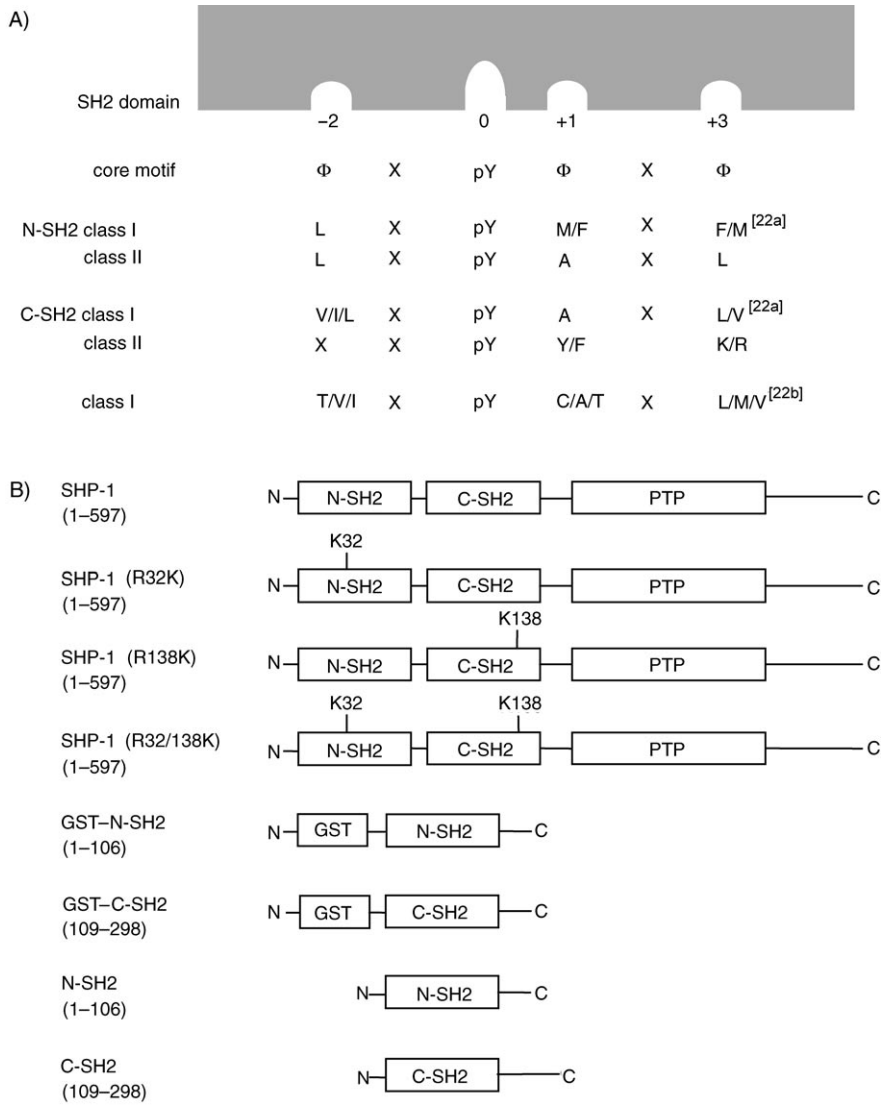

Figure 1. A) Different classes of consensus sequences described for the SH2 domains of SHP-1[22] and B) SHP-1 and SH2 domain constructs used in this study.

Knowledge of the structural features of SH2 domain–ligand interactions is a prerequisite for the development of antagonists of SH2 domain binding. The screening of phosphopeptide libraries revealed different classes of consensus sequences for the SHP-1 SH2 domains (Figure 1 A).[22]

We previously elucidated the requirements for high-affinity binding to the SHP-1 N-SH2 domain by introducing conformationally restricted amino acids and side-chain–side-chain cyclization in peptides derived from a segment of the epithelial receptor tyrosine kinase Ros.[23] Most interestingly, two cyclic peptides (compounds **2** and **3**, Table 1) obtained from this study were found to bind to the N-SH2 domain, but they did not activate the enzyme, and even partially prevented the stimulation of SHP-1 activity by the physiological ligand Ros pY2267 (**1**). In the present study, we sought to corroborate our modeling-derived hypothesis that this behavior might result from an imperfect fit of the amino acid side chains that occupy the SH2 domain pockets pY+1 and pY+3. Furthermore, we explored the contribution of each individual SH2 domain to the activation of SHP-1 by pY ligand-binding studies.

Results and Discussion

We recently reported the design, synthesis, and biological evaluation of a series of linear and cyclic phosphopeptides for the

Table 1. Characterization of the phosphopeptides synthesized.

Peptide	Sequence	M_w [g mol^{-1}][a]	t_R [min][b]	R_{f1}/R_{f2}[c]
1[d]	EGLNpYMVL-NH_2 (Ros pY2267)	1016.8	20.62	0.48/0.48
2	EGLKpYMDL-NH_2 (CO-CH_2-NH)	1109.5	18.80	0.45/0.57
3	EGLKpYMEL-NH_2 (CO-CH_2-NH)	1101.4	19.40	0.47/0.59
4	EGLNpYFV-Hfe-NH_2	1104.6	27.43	0.47/0.60
5	EGLNpY-Nle-V-Hfe-NH_2	1070.7	26.80	0.46/0.57
6	EGLNpYAVL-NH_2	996.5	17.45	0.42/0.46
7	EGLKpYFD-Hfe-NH_2 (CO-CH_2-NH)	1173.0	26.50	0.45/0.57
8	EGLKpY-Nle-D-Hfe-NH_2 (CO-CH_2-NH)	1138.8	25.10	0.45/0.60
9	EGLKpYADL-NH_2 (CO-CH_2-NH)	1032.0	15.60	0.39/0.48

[a] Molecular weight values were determined as $[M+H]^+$, $[M+Na]^+$, or $[M+K]^+$. [b] Conditions: 10→50% eluent B over 40 min (eluent A: 0.1% TFA/water, eluent B: 0.1% TFA/acetonitrile), flow rate: 1.0 mL min^{-1}, detection: $\lambda = 220$ nm. [c] System 1: *n*-butanol/acetic acid/water (48:18:24); system 2: pyridine/ethyl acetate/acetic acid/water (5:5:1:3). [d] Data were reported previously.[23]

N-terminal SH2 domain of SHP-1.[23,24] Compounds **2** and **3** had an inhibitory effect on the stimulation of SHP-1 activity which, in contrast to activating ligands, only partially occupied one of the major SH2 domain pockets (pY + 3) shown in Figure 1 A. To find the structural determinants for N-SH2-directed inhibitors of SHP-1 activity, we focused on a new series of peptides (Table 1), which contain optimal residues at pY + 1 and pY + 3 as determined in preliminary studies.[22,23] Apart from the evaluation of their capacity to stimulate SHP-1 activity (phosphatase assay), and to bind to the N-SH2 domain (SPR measurements), we performed phosphatase assays with mutated forms of SHP-1 (Figure 1 B) to investigate the contribution of each SH2 domain to the activation of the phosphatase.

Competitive binding assay

Based on our recent observation that the cyclic peptides **2** and **3** inhibited Ros pY2267-stimulated SHP-1 activity,[23] we hypothesized that both peptides might compete with the native ligand **1** for association with the N-SH2 domain (Table 2). To test this hypothesis, we assessed the putative competition by binding assays. Binding of the N-SH2 domain to Ros pY2267 was examined after the incubation of the protein with different concentrations of the cyclic peptides prior to the SPR measurements. Competition was readily detectable in this assay as an inhibition of binding. The native Ros pY2267 peptide served as a positive control.

These studies revealed an IC_{50} value of 0.32 μM for peptide **2**, whereas for peptide **3** an IC_{50} value of 0.71 μM was found (Figure 2 A). The lower efficacy of peptide **2** relative to that of **3** in the competition corresponds to the dissociation constant (K_D) values that were previously obtained for both compounds

Table 2. Half-maximal activation and dissociation constants for the phosphopeptides investigated herein.

Peptide	EC_{50} [μM]	K_D [μM][a]	K_D [μM][b]
1	160[c]	1.44 ± 0.45	2.44 ± 0.97
2	N.A.[d]	0.11 ± 0.01	1.01 ± 0.19
3	N.A.	0.21 ± 0.07	1.35 ± 0.13
4	17	0.09 ± 0.01	N.D.[e]
5	47	0.11 ± 0.15	N.D.
6	124	0.39 ± 0.07	1.00 ± 0.48
7	31	0.06 ± 0.01	6.43 ± 1.16
8	49	0.06 ± 0.01	3.33 ± 1.18
9	123	0.70 ± 0.12	1.41 ± 0.61

[a] SPR measurements performed with GST–N-SH2. [b] SPR measurements performed with GST–C-SH2. [c] Data were reported previously.[23] [d] N.A.: not active. [e] N.D.: not determined.

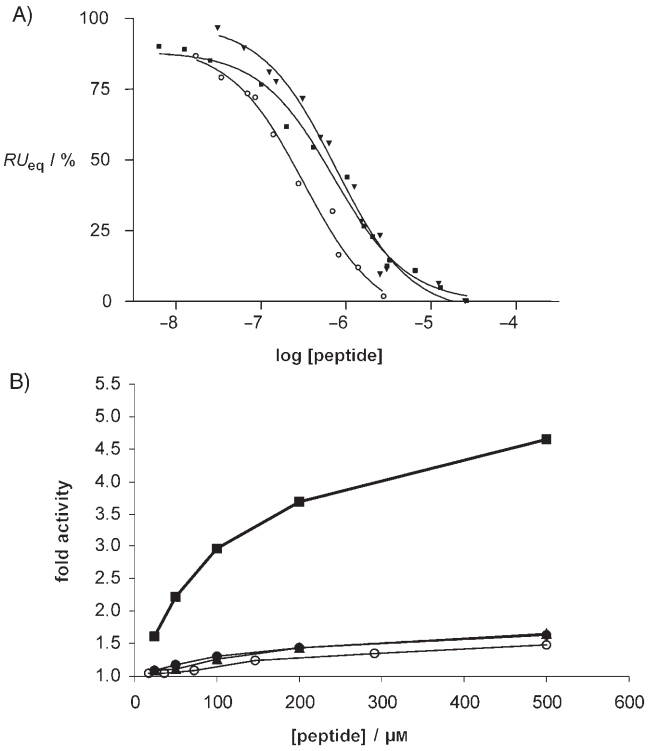

Figure 2. A) Binding of peptide **1** (▼) and cyclic peptides **2** (○) and **3** (■) to the SHP-1 N-SH2 domain. Nonlinear regression analysis was carried out in the one-site binding competition mode. Biotinylated Ros pY2267 was immobilized on a streptavidin-coated sensor chip, and the binding of the protein after 15 min incubation with increasing amounts of peptide was measured (RU_{eq} levels). B) Stimulation of phosphatase activity of the R32K mutant for the peptides **1** (▲), **2** (●), and **3** (○) relative to the stimulation of wild-type SHP-1 by **1** (■). The results are given relative to the basal activity (without peptide).

(0.11 ± 0.01 and 0.21 ± 0.07 μM, respectively).[23] Thus, both cyclic peptides indeed compete directly with the native ligand for binding to the N-SH2 domain, and the smaller ring size in **2** (20 atoms) is favored over **3** (21 atoms). However, according to the results of the competitive phosphatase assay, both peptides inhibited the stimulation of SHP-1 phosphatase activity by Ros pY2267 only at low concentrations (25–50 μM), whereas

at higher concentrations a weak activating effect dominated. We speculated that this might be due to the additional engagement of the C-SH2 domain.[23] To test this possibility, we analyzed the activation of an SHP-1 variant with the mutated (R32K) N-SH2 domain. This mutation at the site of the SH2-domain-conserved Arg residue, which is located on the bottom of the pY-binding pocket (βB5 position), abrogates most of the phosphopeptide binding capacity.[25] However, some binding is retained, and this mutant can still be partially stimulated by phosphopeptides, as reported earlier by Pei et al.[26] As shown in Figure 2B, similarly modest activation of the SHP-1 R32K mutant was detectable for the native ligand **1**, as well as for compounds **2** and **3**. Thus, activation of SHP-1 by the C-SH2 domain does not appear to play a role for the observed pattern of interaction for compounds **2** and **3** with SHP-1.

Synthetic considerations for new pY ligands

Another explanation for the partial antagonist properties of compounds **2** and **3** relates to the structural requirements for SHP-1 activation. Stimulation of SHP-1 activity presumably requires optimal occupation of the N-SH2 domain pockets pY+1 and pY+3 by the amino acid side chains of the ligand; this is not the case for cyclic compounds **2** and **3**. Therefore, the allosteric conformational change within the N-SH2 domain, which is required for the release of the phosphatase domain, is insufficient in the presence of **2** and **3** relative to that elicited by the highly active linear peptides identified earlier (Figure 1A). These contained norleucine (Nle), Phe, or L-α-amino-β-phenylbutyric acid (L-Abu(βPh)) in position pY+1 and homophenylalanine (Hfe), L-Abu(βPh) or L-β-phenylserine (L-Ser(βPh)) in pY+3.[23] Cyclic peptides containing these amino acids might, in contrast to **2** and **3**, be able to stimulate SHP-1 phosphatase activity because of an optimal binding in these SH2 domain pockets. Similarly, linear peptides containing combinations of these preferred amino acids will probably result in highly efficient activators of SHP-1 activity.

The non-proteinogenic amino acids Abu(βPh) and Ser(βPh) are only available as racemic mixtures. The separation of these peptides was very time-consuming and complex.[24] Therefore, to check our hypotheses, we decided to incorporate only the residues Phe/Nle and Hfe at pY+1 and pY+3, respectively. Also, the improved binding affinity of **2** over **3** led us to introduce Asp instead of Glu in the cyclic peptides. This resulted in the preparation of the linear compounds **4** and **5**, and the corresponding cyclic peptides **7** and **8** (Table 1). Furthermore, we synthesized peptides **6** and **9**, which correspond to the consensus class II,[22] to evaluate the effects of the different recognition motifs on the binding and the stimulation of phosphatase activity, particularly with regard to the cyclic peptides (Table 1).

Stimulation of SHP-1 activity

The ability of the pY-containing peptides to stimulate SHP-1 activity was examined at neutral pH using *p*-NPP as the substrate. In addition to the assay with the wild-type enzyme, we used SHP-1 mutants (Figure 1B) to determine whether there are differences in the binding and activation evoked by the linear and cyclic peptides. As shown in Figure 3, all peptides

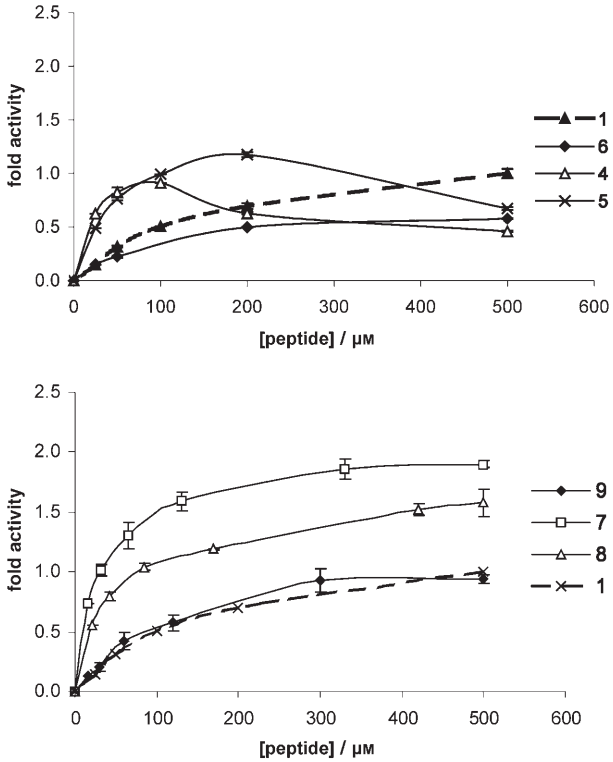

Figure 3. Concentration-dependent stimulation of SHP-1 activity by the peptides synthesized for this study (see Tables 1 and 2). The results are given relative to the activity of SHP-1 stimulated by Ros pY2267.

indeed showed an efficient stimulation of wild-type SHP-1. In contrast to Ros pY2267 (**1**), peptide **4** reached half-maximal activation at 17 μM, and compound **5**, at 47 μM. This is in agreement with our expectations that a combination of the optimal residues leads to an increase in potency. These values also exceed those found for the linear peptides containing single amino acid substitutions, described earlier.[23] However, for both peptides an inhibition of phosphatase activity at higher concentrations was observed. A similar curve shape was also obtained for some peptides of the first series, such as EGLN-pYFVF-NH_2.[23]

However, this behavior was not observed for the cyclic peptides that contain the preferred residues at pY+1 and pY+3. Peptide **7** stimulated SHP-1 activity most efficiently, and was also more potent than the lead structure Ros pY2267 (**1**, Figure 3). The trend observed for the cyclic peptides is the same as for the linear activators, as Phe is preferred over Nle at pY+1. Additionally, we found that peptides **7** and **8** stimulate SHP-1 activity even more potently than the most efficient linear counterparts **4** and **5** (with respect to maximal activity). This is most likely due to a combined effect of the rigid backbone and the sterically preferred residues at pY+1 and pY+3.[23]

The linear peptide **6**, which corresponds to the class II consensus sequence (Figure 1A) stimulated SHP-1 activity to a lesser extent than native Ros pY2267. The EC_{50} values for both peptides were similar, whereas the maximal activity at a peptide concentration of 500 μM was higher for Ros pY2267 (**1**) than for **6** (Figure 3). Interestingly, the cyclic counterpart **9** stimulated phosphatase activity similarly to the lead peptide **1**. Peptide **9** only differs from cyclic peptide **2** of our first study in the amino acid at pY+1 (Table 1). Thus, the incorporation of Ala instead of Met at pY+1 in the cyclic scaffold clearly leads to the activation of SHP-1.

Importantly, SHP-1 activation requires efficient peptide binding to the N-SH2 domain and dissociation of the N-SH2 from the PTP domain. This dissociation requires a peptide-induced conformational change of the N-SH2 domain, specifically, the change of a loop conformation as illustrated in Figure 4A. It is likely that this peptide-induced conformational change depends on the peptide-binding mode. Indeed, the crystal structure of SHP-2 N-SH2, which has >50% sequence identity to SHP-1 N-SH2, was determined in a complex with a class I and a class II consensus peptide. These crystal structures indicate significantly different peptide-binding conformations (Figure 4B and D).[28,29] As illustrated in Figure 4C and E, the conformational state that occurs in the free N-SH2 domain of the enzyme inactive form, which is bound to the PTP domain, especially interferes with the pY+3 residue. In particular, the localization of the pY+3 residue in the class II binding mode is sterically incompatible with the N-SH2 conformation that keeps the enzyme inactive (Figure 4C). In contrast, class I-type binding provides more space for conformational changes of the loop formed by N-SH2 residues 62–68 (Figure 4E). Hence, both the binding mode (class I or II) and the nature of the pY+3 residue determine the degree of enzyme activation. For these structural considerations, it is assumed that the mechanism of peptide binding and activation is similar for SHP-1 and SHP-2, as only for the latter the N-SH2 domain crystal structures in the peptide-bound and unbound form are available.[28,29]

A possible explanation for the binding and activation pattern is that the peptide cyclization may shift the binding mode in most cases towards class I-type binding. This assumption is reasonable, as the distance between the two amino acids that enable the cyclization is smaller for the class I mode than it is for the class II mode. The linear lead peptide **1** predominantly binds in a class II binding mode (leading to PTP activation) as reported earlier,[23] whereas the cyclic variants **2** and **3** preferably adopt the class I binding mode. As in these cases the pY+3 residue is small (Leu), no activation is induced. In the case of peptides **4**, **5**, **7**, and **8**, the peptides have large bulky residues at both pY+1 and pY+3 (close to the class I consensus), and all bind in the class I mode. However, in contrast to peptides **2** and **3** (Leu at pY+3), the pY+3 residue is large and bulky (Hfe) and thus does not sterically allow the transition to an N-SH2 conformation that binds to the PTP domain. Consequently, these peptides all activate SHP-1. In the case of peptide **9**, the fact that it resembles the class II consensus sequence might interfere with a transition to the class I binding mode, even in the case of peptide cyclization. Therefore, this sequence binds in the class II mode both in the case of the linear and the cyclic compound and consequently stimulates PTP activity in both cases. The hypothesis is supported by the finding that only in the case of the class II consensus peptide sequences (peptide **6** and **9**) does cyclization lead to a decrease in binding affinity, whereas in all other cases, peptide cyclization enhances the association to SHP-1 N-SH2 (Table 2). This indicates

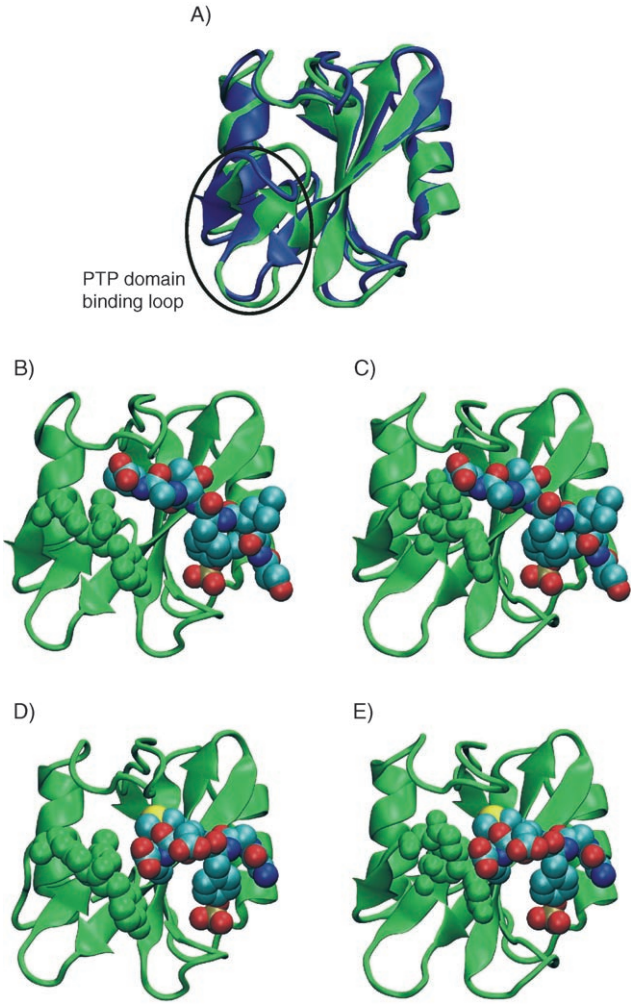

Figure 4. A) Superposition of the N-SH2 domain of SHP-2 in the peptide bound form (blue, PDB code 1aya) and in the empty form (green, extracted from PDB code 2shp). The empty N-SH2 form corresponds to the conformation in complex with the PTP domain of SHP-2 (inactive enzyme). The loop region that contacts the PTP domain and that can undergo an allosteric conformational change upon peptide binding is encircled. B) Peptide binding in class II mode (PDB 1aya) with the pY peptide and the N-SH2 loop residues 65–68 in van der Waals representation and the N-SH2 domain in ribbon representation (green). C) Superposition of the bound pY peptide in the class II binding mode (peptide from PDB 1aya, atomic color code) on the peptide binding region of the empty N-SH2 domain (green). Peptide and loop residues are in van der Waals representation to indicate the steric overlap between the pY+3 residue and the PTP binding loop of the N-SH2 domain. D) and E) same for a peptide binding in the class I mode (extracted from PDB 1ayc). The contact between peptide and the loop region causes less overlap than in case of class II mode binding. The structures shown in C) and E) with peptides docked into the peptide binding region of the empty N-SH2 domain were energy minimized (20 steps) using the SPDBV program.[27]

that the binding mode for peptide **9** might indeed differ from the binding modes of the other cyclic peptides and is destabilized by cyclization.

Activation of SHP-1 mutants

To test whether the activation of SHP-1 is due to an interaction of the phosphopeptides with individual or tandem SH2 domains and to what extent, we repeated the phosphatase assay with selected peptides from our previous study.[23] The assay was also carried out with the pY ligands, which were prepared in the present study, by using SHP-1 SH2 domain mutants (Figure 1B) with single amino acid substitutions (R→K) of the invariant Arg (βB5), which is found in the pY binding pocket of SH2 domains.[30,31] In the epithelial form of SHP-1, these Arg residues are located at positions 32 (N-SH2 domain) and 138 (C-SH2 domain).[32]

To compare the activation of the different SHP-1 forms, the absorption (release of *p*-nitrophenol) at a fixed peptide concentration was determined relative to the corresponding basal activity. In the case of the R138K mutant, a slightly diminished activation was obtained for all phosphopeptides relative to the wild-type enzyme (Figure 5). For example, Ros pY2267 activated SHP-1 R138K 4.3-fold at a concentration of 500 μM, while a 5.1-fold increase in activation was observed with wild-type SHP-1. Among the peptides tested, the same tendency of activation efficiency was observed as was determined for the wild-type SHP-1. For the linear peptides **4** and **5** the highest SHP-1 activity was at concentrations of 100 μM and 200 μM, respectively, whereas higher peptide concentrations led to phosphatase inhibition. The maximal activity induced by either Ros pY2267 or the linear peptides **4** and **5** was exceeded by the cyclic peptides **7** and **8** by 71 and 38%, respectively. In contrast, the stimulation of phosphatase activity of the R138K mutant by the cyclic compounds **2** and **3** was only 45% of the activity obtained for Ros pY2267, which is consistent with their poor capacity to activate the wild-type SHP-1.

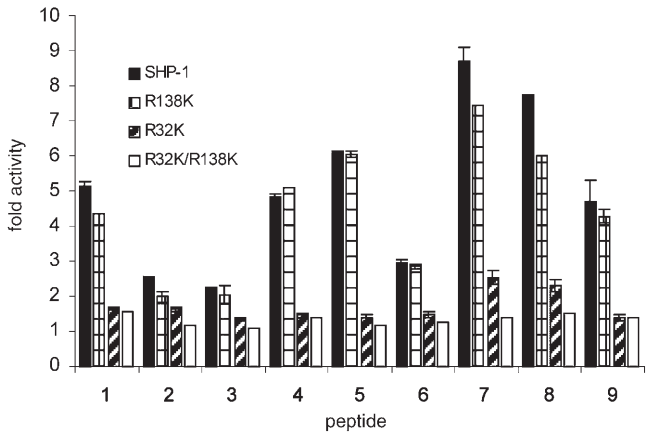

Figure 5. Activity of SHP-1 and mutant forms stimulated by pY ligands (Table 1) at a peptide concentration of 500 μM relative to basal activity (without peptide).

The maximal activity obtained for the R32K mutant of SHP-1 was greatly diminished for all peptides relative to wild-type enzyme (Figure 5), which indicates that the interaction of the phosphopeptides with the N-SH2 domain is essential for activation. As discussed above, the remaining activation of this mutant probably relates to the residual capacity of the N-SH2 domain for binding phosphopeptides. In agreement with this assumption, the ranking of the peptides for this residual activation was the same as for the wild-type SHP-1. Further, peptides **4** and **5** showed the same activation profile for R32K as for the intact enzyme. The most potent compounds with respect to maximal activity were the cyclic peptides **7** and **8**, as was found for the wild-type enzyme. Peptides **6** and **9**, corresponding to the class II consensus sequence, activated R32K SHP-1 to a lesser extent than Ros pY2267.

In conclusion, these results indicate that the interaction of the pY ligands with the C-SH2 domain plays only a minor role in the stimulation of SHP-1 activity, although at least some of the phosphopeptides displayed appreciable binding affinity for the C-SH2 domain (Table 1, see below).

As expected, the activation of the R32/138K mutant was also strongly diminished, similar to the case of the R32K mutant. A maximal activity of $<30\%$ was found for Ros pY2267 (Figure 5). In general, the activation of this mutant by peptides **2**–**9** was only in the range of 20–27%, and thus was lower than for R32K, R138K, and wild-type SHP-1. However, this level of SHP-1 activity is still induced by the recognition of specificity determinants outside pY.

Kinetic analysis of the Ros pY2267–N-SH2-domain interaction

We initially determined K_D values for the interaction of phosphopeptides with the GST-conjugated SHP-1 N-SH2 domain by using surface plasmon resonance (SPR) spectroscopy.[23] However, it was described earlier that avidity effects, which result from the dimerization of GST fusion proteins with SH2 domains, can lead to overestimates of the binding affinities.[33] Furthermore, modifications of the binding kinetics due to an influence of the fusion partner (GST) were also discussed.[34] To evaluate the influence of the GST tag on the SPR-derived K_D values, we compared binding experiments for the lead peptide **1** with the free SHP-1 N-SH2 domain and GST–N-SH2. Although the K_D values were similar for the GST–SH2 fusion protein and the isolated SH2 domain, we observed differences in the k_{on} and k_{off} rates, indicating distinctions in the binding kinetics (Figure 6). For the free N-SH2 domain, high k_{on} and k_{off} rates were observed, corresponding to very fast respective association and dissociation events relative to those with the GST–SH2 fusion protein. A reasonable explanation for this fact is that GST (26 kDa) hampers the binding of the interaction partners because of a restriction of the flexibility and accessibility of the protein domain. However, the K_D values determined for **1** (GST–N-SH2: 1.44 ± 0.45 μM; N-SH2: 1.32 ± 0.16 μM) confirm that the fusion to GST does not influence the interaction of phosphopeptides to the SH2 domain. This is consistent with the data reported for the binding of phosphopeptides to both

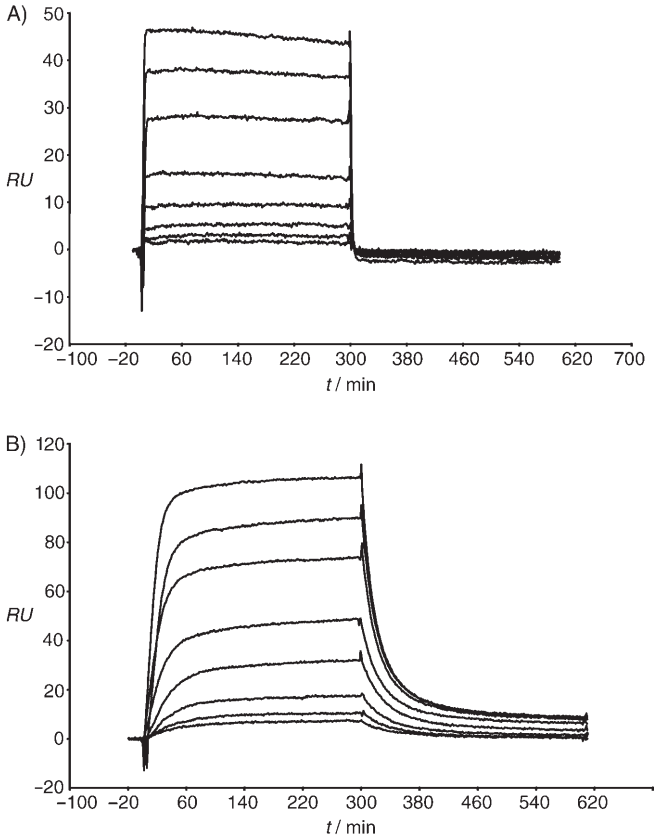

Figure 6. SPR sensorgrams of SHP-1 N-SH2 binding to Ros pY2267 (**1**, EGLN-pYMVL): A) isolated N-SH2 domain; B) GST–N-SH2 fusion protein. The concentration of the phosphopeptide on the sensor chip corresponded to 25–30 *RU*; protein concentrations ranged from 13 to 1 μM.

the isolated and GST-conjugated SH2 domain of Src.[33] Furthermore, our results are in good agreement with the K_D values for pY ligand binding to the His_6-tagged SH2 domains of SHP-1, which were reported earlier.[22] Thus, we decided to proceed with the analysis of the other phosphopeptides using the GST fusion proteins for SPR analysis.

Binding affinities of pY ligands for SHP-1 N-SH2

To evaluate whether the increased phosphatase activity obtained for the pY ligands described herein is caused by a higher binding affinity for the N-SH2 domain, we determined the K_D values by SPR. The linear peptides **4** (Phe, Hfe) and **5** (Nle, Hfe), containing substitutions at pY+1 and pY+3, displayed lower K_D values (0.09±0.01 and 0.11±0.05 μM, respectively) than the peptides of the previous study, which carried only one modification at either position: for example, EGLN-pY**F**VL-NH_2 (0.69±0.21 μM) and EGLNpYMV**Hfe**-NH_2 (0.27±0.10 μM) (Table 2).[23] The cyclic peptides **7** and **8** showed the highest affinity for SHP-1 N-SH2 (0.06±0.01 μM) of all peptides tested, indicating an optimal fit of both the pY+1 and pY+3 amino acids and the backbone conformation of the ligand into the protein binding site. These data provide further evidence for the hypothesis that beside the backbone conformation of the ligand, the bulky pY+3 residue (Hfe) of compounds **4**, **5**, **7**, and **8** contributes to the conformational change in the N-SH2 domain. This finally leads to activation of the phosphatase (see Figure 4).

The linear and cyclic ligands corresponding to the class II consensus sequence **6** and **9** also reached lower K_D values than did the native ligand **1**. Again, this is due to their association in the class II binding mode, which is preferred over class I binding with respect to binding affinity (Figure 4).[22,23]

Binding affinities of pY ligands for SHP-1 C-SH2

The binding affinities of selected phosphopeptides to the C-SH2 domain were lower than those determined for the N-SH2 domain in all cases (Table 2). In general, the affinity data were confirmed by the kinetic values in the SPR measurements. A comparison of the kinetic data for the binding of the peptides to the GST–C-SH2 domain revealed a greater than 10-fold decrease in k_{on} and k_{off} values for these interactions (GST–N-SH2: $k_{on}=0.04–1.6\times10^5$, $k_{off}=6.8–15.3\times10^{-3}$, GST–C-SH2: $k_{on}=4.8–16\times10^2$, $k_{off}=0.8–3\times10^{-3}$), indicating slower association and dissociation of the ligand–protein complex. The K_D value of the lead peptide **1** for the GST–C-SH2 domain is about 1.7-fold higher than that of the GST–N-SH2 domain (2.44±0.97 versus 1.44±0.45 μM). The cyclic peptides **2** and **3** displayed lower K_D values than Ros pY2267 (Table 1), similar to the case of the N-SH2 domain. The cyclic peptides **7** and **8**, which represent N-SH2 class I consensus sequence (Figure 1 A) were less potent than all of the other peptides tested. Evidently, the interactions of the peptide side chains at pY+1 and pY+3 hamper the association of the protein to the C-SH2 domain; moreover, this consensus is not generally preferred by SHP-1 C-SH2.[22] Although both domains showed similarities in the sequence specificity, class II of the C-SH2 domain (XXpYY/FMK/R) especially differs from the N-SH2 class I (LXpYM/FXF/M). The peptides corresponding to N-SH2 class II (**6** and **9**) appear to be optimal interaction partners for the C-SH2 domain, in good agreement with the literature.[22] The K_D values for the linear compound **6** and the cyclic **9** were in the range of the cyclic peptides **2** and **3**, and were therefore clearly independent of cyclization. Also, similar to the results obtained for the GST–N-SH2 domain, the cyclization within peptide **9** did not improve the affinity over the linear counterpart of this class of consensus sequence.

Conclusions

The study reported herein was predicated on previous findings that cyclization within the SHP-1 native interaction partner Ros pY2267 (**1**, EGLNpYMVL) leads to compounds (**2** and **3**) with potentially enhanced N-SH2 binding affinity and with the ability to partially inhibit the Ros pY2267-mediated activation of SHP-1.[23] On the basis of these results, it has been hypothesized that in the corresponding peptides, a backbone conformation close to the bound form is stabilized, but the binding geometry of the pY+1 and pY+3 residues is concomitantly distorted. Thus, our objective was to identify the origin of the

high affinity and the inhibitory effect of **2** and **3** by a new series of pY ligands.

More precisely, we focused on three experiments: 1) the incorporation of optimal residues at the pY+1 and pY+3 positions in both linear and cyclic compounds to check their importance for SHP-1 activation,[23] 2) the introduction of consensus sequence class II in a linear and cyclic peptide to evaluate the effects of different recognition motifs on SHP-1 binding and activation, and 3) the use of SHP-1 mutants containing replacements of the highly conserved Arg residue (R→K) in the FLVRE motif of either or both SH2 domains to estimate the contribution of each SH2 domain on activation or inhibition of SHP-1.

Consistent with our hypotheses, we found that linear peptides **4** and **5** were more potent in stimulating SHP-1 activity than the native Ros pY2267, although the introduction of the bulky residues (Phe, Nle, Hfe) in the cyclic peptides **7** and **8** gave rise to even greater efficiency, especially in terms of binding to the N-SH2 domain. Interestingly, the introduction of the class II consensus sequence in the context of a linear peptide (compound **6**) and a cyclic peptide (compound **9**) increased the binding affinity and also the ability to stimulate SHP-1 activity relative to the native ligand **1**. However, **6** and **9** were not as efficient as the optimized compounds **4**, **5**, **7** and **8**. In contrast to compounds **4**–**9**, peptides **2** and **3** bind efficiently without activating the phosphatase. These peptides evidently associate with the protein in a mode that allows a conformational state of SHP-1 N-SH2 which is suitable to inhibit the phosphatase domain.[23,28] We suggest that peptide cyclization leads to a switch in the peptide binding mode toward the class I mode with a "bent" peptide conformation (Figure 4) that provides greater conformational freedom of a loop segment that is involved in the interaction with the phosphatase domain. In contrast, peptides **4**–**9** presumably bind in the class II mode, leading to PTP activation. Depending on the sequence, it is also possible that peptide cyclization may cause an imperfect steric fit at the pY+3 binding region, thus allowing greater conformational freedom of peptides with smaller residues (**2** and **3**) than for peptide sequences with bulky residues (**7** and **8**) at this position. Ultimately, X-ray crystal structure analysis of the N-SH2 domain in a complex with selected cyclic peptides described herein would allow us to identify possible differences in the binding modes of these peptides.

To assess whether the inhibitory effect of peptides **2** and **3** is mediated through either the individual (N- or C-terminal) or both (N+C) SH2 domains, we analyzed the stimulation of phosphatase activity with the corresponding (R→K) point mutants. Consistent with published data,[17] the C-SH2 domain plays only a minor role in enzyme activation, and the effects of **2** and **3** relative to the lead peptide **1** on PTP activation were not as significant for the C-SH2 domain as they were for N-SH2. We therefore conclude that these peptides mediate their inhibitory action mainly through the N-SH2 domain. Ongoing studies are concentrated on replacing the elements for cyclization and the bridging unit to obtain more potent inhibitors of SHP-1 activity.

Experimental Section

General: All chemicals used were of reagent grade from Fluka (Sigma–Aldrich, Taufkirchen, Germany). Fmoc-protected amino acids, coupling reagents (HBTU, HOBt, PyBOP, DCC) and Rink amide MBHA resin were purchased from Novabiochem (Merck Biosciences AG, Schwalbach, Germany) and Orpegen (Heidelberg, Germany). Solvents for chromatography were of analytical grade from Acros Organics (Geel, Belgium) or VWR International GmbH (Dresden, Germany). Biomol green solution was obtained from Biomol GmbH (Hamburg, Germany). Glutathione Sepharose High-Performance and GSTrapp FF columns were purchased from Amersham Biosciences (Freiburg, Germany). The GST fusion proteins were cleaved by using protease factor Xa (New England Biolabs, Frankfurt/Main, Germany). The Streptavidin-coated sensor chips were from Biacore International SA (Freiburg, Germany).

Peptide synthesis: Solid-phase peptide synthesis was carried out manually on a Rink amide MBHA resin (0.64 mmol g^{-1}) using syringes from Abimed (Langenfeld, Germany). The peptides were synthesized using a standard Fmoc protocol as previously described.[23,24] The side chains of the trifunctional amino acids were protected as follows: Asn(Trt), Glu(O*t*Bu), Tyr(PO_3H_2) (for linear peptides) and Tyr[PO(OBzl)OH] (for cyclic peptides). For the cyclization procedure Alloc and OAll side chain protecting groups were used (Fmoc-Asp(Gly-OAll)-OH, Fmoc-Lys(Alloc)-OH). The deprotection of the Alloc/OAll groups was carried out with DMF (2 mL), THF (2 mL), 0.5 N HCl (1 mL), morpholine (900 μL), and [$Pd(PPh_3)_4$] as the catalyst for 500 mg resin. The reaction time was 16 h. Cyclization was performed using PyBop as described earlier.[24] The peptides were synthesized as N-terminal unprotected sequences for the phosphatase assay and in the biotinylated form for the SPR binding studies.[23,24]

Purification and characterization of peptides: Peptide purification was performed on a semipreparative reversed-phase HPLC using a Shimadzu LC-8A system equipped with a C18 column (Knauer Eurospher 100, Berlin, Germany) with a gradient from 15 to 65% eluent B over 120 min at a flow rate of 10 mL min^{-1} (A: 0.1% TFA in water; B: 0.1% TFA in 90% acetonitrile/water). Detection was performed at $\lambda = 220$ nm. Analytical RP HPLC was performed on a Shimadzu LC-10AT chromatograph (Duisburg, Germany) with a Vydac 218TP column (4.6×25 mm, particle size 5 μm, pore size 300 Å) and a binary mobile phase system consisting of A: 0.1% TFA in water and B: 0.1% TFA in acetonitrile at a gradient of 10 to 50% eluent B over 60 min at a flow rate of 1.0 mL min^{-1}; detection at $\lambda = 220$ nm. The molecular weight values of the peptides were determined by MALDI-TOF MS on a Laser Tec Research mass spectrometer (Perspective Biosystems, Weiterstadt, Germany). The peptides were characterized by TLC on precoated plates of silica gel 60 F_{254} (Merck, Darmstadt, Germany) (Table 1).

The concentration of the peptide solutions was determined by quantitative amino acid analysis and the malachite green assay for inorganic phosphate, as previously described.[23,24]

Expression and purification of recombinant proteins: Full-length SHP-1, N-SH2, and C-SH2 domains as well as mutants of SHP-1[32] (Figure 1 B) were expressed as GST fusion proteins using the pGEX-5X1 expression vector system. Expression by transformed *E. coli* BL21(DE3)pLys cells was induced by the addition of isopropyl thiogalactoside (IPTG, 250 μM). Purification was performed as described earlier.[32] The GST tag was cleaved by treatment with factor Xa (1:50) and SHP-1 was subsequently purified as reported.[32] For the SPR measurements, the proteins were additionally purified by gel filtration (Pharmacia LKB GP-10, Pharmacia LKB Biotechnology

AB, Uppsala, Sweden) equipped with a Sephacryl 16/60 S-100 high-resolution column (Amersham Bioscience, Uppsala, Sweden). The protein concentrations were determined by absorbance measurements at $\lambda = 280$ nm and by the Bradford method using Roti-Nanoquant (Carl Roth GmbH, Karlsruhe, Germany) with bovine serum albumin as standard.

Phosphatase assay: Peptides were diluted in assay buffer (100 mM HEPES, pH 7.4, 150 mM NaCl, 1.0 mM EDTA, 20 mM DTT) to obtain the final assay concentrations of 25, 50, 100, 200 and 500 μM. The stimulation of the activity of full-length SHP-1 and of the different mutants was measured using *p*-nitrophenylphosphate (*p*-NPP) as substrate. The assay was carried out in a final reaction volume of 50 μL. The reaction was initiated by the addition of SHP-1 or SHP-1 mutant (final concentration: 15 nM), and was allowed to proceed for 30 min at room temperature. The reaction was quenched by adding 1.0 M NaOH (100 μL). Absorbance was then measured at 405 nm on a VERSA max (Molecular Devices GmbH, Ismaning, Germany). The results were determined either relative to activation by Ros pY2267 (**1**), or relative to the basal activity. All measurements were carried out in duplicate, and the results are given as mean value ±SD of two different experiments.

SPR measurements: SPR measurements were carried out on a Biacore 2000 instrument (Pharmacia Biosensor AB, Uppsala, Sweden). A streptavidin-coated sensor chip (Biacore International SA, Freiburg, Germany) was conditioned with 1.0 M NaCl/50 mM NaOH according to the instructions of the manufacturer. All reactions were carried out at room temperature in HBS buffer (10 mM HEPES, pH 7.4, 150 mM NaCl, 3.4 mM EDTA, 0.005% Tween 20). Affinity measurements were made as previously described.[23] The data were analyzed with BIAevaluation 2.0 software. To determine the dissociation constant (K_D), the equilibrium response units (RU_{eq}) were plotted against protein concentration and fit to the equation $RU_{eq} = RU_{max}[\text{protein}]/(K_D + [\text{protein}])$, for which RU_{max} is the maximum response unit. In addition, we estimated the rate constants of association (k_{on}) dissociation (k_{off}) with a nonlinear least-squares method. The competitive binding (IC_{50} values) of the cyclic ligands to the GST–N-SH2 domain was determined by mixing increasing concentrations (31 nM to 50 μM) of the peptides with a constant amount of the GST protein (1.0 μM) for 15 min, and subsequently measuring the binding at equilibrium to immobilized biotinylated Ros pY2267. The RU_{eq} values were compared with the value obtained without cyclic peptide. By using GraphPadPrism 2.0 software, the relative RU_{eq} levels were plotted against the log of the peptide concentrations, and IC_{50} values were calculated from nonlinear regression analysis in the one-site binding competition mode.

Abbreviations: GST, glutathione S-transferase; *p*-NPP, *para*-nitrophenyl phosphate; PTK, protein tyrosine kinase; PTP, protein tyrosine phosphatase; RTK, receptor tyrosine kinase; SH2, Src homology 2; SHP-1, SH2-containing protein tyrosine phosphatase 1.

Acknowledgements

The financial support by the Deutsche Forschungsgemeinschaft (Collaborative Research Center SFB 604, project A1 to F.D.B.), the Fonds der Chemischen Industrie (to D.I.) and the Friedrich-Schiller-Universität Jena (grant to D.I.) is gratefully acknowledged. We thank Professor F. Große (FLI Jena) for the provision of facilities.

[1] B. G. Neel, N. K. Tonks, *Curr. Opin. Cell Biol.* **1997**, *9*, 193–204.
[2] L. Li, J. E. Dixon, *Semin. Immunol.* **2000**, *12*, 75–84.
[3] J. den Hertog, *EMBO Rep.* **2003**, *4*, 1027–1032.
[4] R. H. van Huijsduijnen, A. Bombrun, D. Swinnen, *Drug Discovery Today* **2002**, *7*, 1013–1019.
[5] J. Yang, L. Liu, D. He, X. Song, Z. J. Zhao, G. W. Zhou, *J. Biol. Chem.* **2003**, *278*, 6516–6520.
[6] J. Plutzky, B. G. Neel, R. D. Rosenberg, *Proc. Natl. Acad. Sci. USA* **1992**, *89*, 1123–1127.
[7] H. W. Tsui, K. A. Siminovitch, L. de Souza, F. W. Tsui, *Nat. Genet.* **1993**, *4*, 124–129.
[8] J. S. Bignon, K. A. Siminovitch, *Clin. Immunol. Immunopathol.* **1994**, *73*, 168–179.
[9] H. Keilhack, M. Müller, S. A. Böhmer, C. Frank, K. M. Weidner, W. Birchmeier, T. Ligensa, A. Berndt, H. Kosmehl, B. Günther, T. Müller, C. Birchmeier, F. D. Böhmer, *J. Cell Biol.* **2001**, *152*, 325–334.
[10] N. R. Paling, M. J. Welham, *Blood* **2005**, *105*, 4290–4297.
[11] J. Zhang, A. K. Somani, K. A. Siminovitch, *Semin. Immunol.* **2000**, *12*, 361–378.
[12] N. Tidow, B. Kasper, K. Welte, *Exp. Hematol.* **1999**, *27*, 1038–1045.
[13] T. Oka, M. Ouchida, M. Koyama, Y. Ogama, S. Takada, Y. Nakatani, T. Tanaka, T. Yoshino, K. Hayashi, N. Ohara, E. Kondo, K. Takahashi, J. Tsuchiyama, M. Tanimoto, K. Shimizu, T. Akagi, *Cancer Res.* **2002**, *62*, 6390–6394.
[14] M. F. Johan, D. T. Bowen, M. E. Frew, A. C. Goodeve, J. T. Reilly, *Br. J. Haematol.* **2005**, *129*, 60–65.
[15] A. Beghini, C. B. Ripamonti, P. Peterlongo, G. Roversi, R. Cairoli, E. Morra, L. Larizza, *Hum. Mol. Genet.* **2000**, *9*, 2297–2304.
[16] J. Yang, X. Liang, T. Niu, W. Meng, Z. Zhao, G. W. Zhou, *J. Biol. Chem.* **1998**, *273*, 28199–28207.
[17] D. Pei, J. Wang, C. T. Walsh, *Proc. Natl. Acad. Sci. USA* **1996**, *93*, 1141–1145.
[18] D. N. Burshtyn, W. Yang, T. Yi, E. O. Long, *J. Biol. Chem.* **1997**, *272*, 13066–13072.
[19] C. Frank, H. Keilhack, F. Opitz, O. Zschornig, F. D. Böhmer, *Biochemistry* **1999**, *38*, 11993–12002.
[20] Z. Zhang, K. Shen, W. Lu, P. A. Cole, *J. Biol. Chem.* **2003**, *278*, 4668–4674.
[21] C. Frank, C. Burkhardt, D. Imhof, J. Ringel, O. Zschörnig, K. Wieligmann, M. Zacharias, F. D. Böhmer, *J. Biol. Chem.* **2004**, *279*, 11375–11383.
[22] a) K. D. Beebe, P. Wang, G. Arabaci, D. Pei, *Biochemistry* **2000**, *39*, 13251–13260; b) M. C. Sweeney, A.-S. Wavreille, J. Park, J. P. Butchar, S. Tridandapani, D. Pei, *Biochemistry* **2005**, *44*, 14932–14947.
[23] D. Imhof, K. Wieligmann, K. Hampel, D. Nothmann, M. S. Zoda, D. Schmidt-Arras, M. Zacharias, F. D. Böhmer, S. Reissmann, *J. Med. Chem.* **2005**, *48*, 1528–1539.
[24] D. Imhof, D. Nothmann, M. S. Zoda, K. Hampel, J. Wegert, F. D. Böhmer, S. Reissmann, *J. Pept. Sci.* **2005**, *11*, 390–400.
[25] M. J. Eck, S. E. Shoelson, S. C. Harrison, *Nature* **1993**, *362*, 87–91.
[26] D. Pei, U. Lorenz, U. Klingmüller, B. G. Neel, C. T. Walsh, *Biochemistry* **1994**, *33*, 15483–15493.
[27] N. Guex, M. C. Peitsch, *Electrophoresis* **1997**, *18*, 2714–2723.
[28] P. Hof, S. Pluskey, S. Dhe-Paganon, M. J. Eck, S. E. Shoelson, *Cell* **1998**, *92*, 441–450.
[29] H.-E. Lee, D. Kominos, S. Jacques, B. Margolis, J. Schlessinger, S. E. Shoelsen, J. Kuriyan, *Structure* **1994**, *2*, 423–438.
[30] M. B. Yaffe, *Nat. Rev. Mol. Cell Biol.* **2002**, *3*, 177–186.
[31] B. J. Mayer, P. K. Jackson, R. A. Van Etten, D. Baltimore, *Mol. Cell. Biol.* **1992**, *12*, 609–618.
[32] H. Keilhack, T. Tenev, E. Nyakatura, J. Godovac-Zimmermann, L. Nielsen, K. Seedorf, F. D. Böhmer, *J. Biol. Chem.* **1998**, *273*, 24839–24846.
[33] J. E. Ladbury, M. A. Lemmon, M. Zhou, J. Green, M. C. Botfield, J. Schlessinger, *Proc. Natl. Acad. Sci. USA* **1995**, *92*, 3199–3203.
[34] M. M. Morelock, R. H. Ingraham, R. Betageri, S. Jakes, *J. Med. Chem.* **1995**, *38*, 1309–1318.

Keywords: hydrolases · SH2 domain ligands · SHP-1 · structure–activity relationships · tyrosine phosphatases

Received: February 15, 2006
Published online on August 31, 2006

